

Journal of Turbomachinery Journal

Copy of e-mail Notification

Journal of Turbomachinery Published by ASME

Dear Author,

Congratulations on having your paper accepted for publication in the ASME Journal Program.

Your page proof is available in PDF format from the ASME Proof Download & Corrections site here:

<http://115.111.50.156/jw/AuthorProofLogin.aspx?pwd=ae0a06d18aa5>

Login: your e-mail address

Password: ae0a06d18aa5

Please keep this email in case you need to refer back to it in the future.

You will need Adobe Acrobat Reader software to view the file. This is free software and a download link is provided when you log in to view your proofs.

Responsibility of detecting errors rests with the author. Please review the page proofs carefully and:

- 1) Answer any queries on the first page "Author Query Form"
- 2) Proofread any tables and equations carefully
- 3) Check to see that any special characters have translated correctly

RETURNING CORRECTIONS:

To return corrections, please use the ASME Proof Download & Corrections Submission Site (link above) and provide either:

1. Annotated PDF
2. Text entry of corrections, with line numbers, in the text box provided

Additional files, as necessary, can also be uploaded through the site.

SPECIAL NOTES:

Your Login and Password are valid for a limited time. Please reply within 48 hours. Your prompt attention to and return of page proofs will speed the publication of your work.

For all correspondence, please include your article no. (TURBO-12-1213) in the subject line.

This e-proof is to be used only for the purpose of returning corrections to the publisher.

If you have any questions, please contact: asme.cenveo@cenveo.com.

Sincerely,

Mary O'Brien, Journal Production Manager

STATEMENT OF EDITORIAL POLICY AND PRACTICE

The Technical Committee on Publications and Communications (TCPC) of ASME aims to maintain a high degree of technical, literary, and typographical excellence in its publications. Primary consideration in conducting the publications is therefore given to the interests of the reader and to safeguarding the prestige of the Society.

To this end the TCPC confidently expects that sponsor groups will subject every paper recommended by them for publication to careful and critical review for the purpose of eliminating and correcting errors and suggesting ways in which the paper may be improved as to clarity and conciseness of expression, accuracy of statement, and omission of unnecessary and irrelevant material. The primary responsibility for the technical quality of the papers rests with the sponsor groups.

In approving a paper for publication, however, the TCPC reserves the right to submit it for further review to competent critics of its own choosing if it feels that this additional precaution is desirable. The TCPC also reserves the right to request revision or condensation of a paper by the author or by the staff for approval by the author. It reserves the right, and charges the editorial staff, to eliminate or modify statements in the paper that appear to be not in good taste and hence likely to offend readers (such as obvious advertising of commercial ventures and products, comments on the intentions, character, or acts of persons and organizations that may be construed as offensive or libelous), and to suggest to authors rephrasing of sentences where this will be in the interest of clarity. Such rephrasing is kept to a minimum.

Inasmuch as specific criteria for the judging of individual cases cannot, in the opinion of the TCPC, be set up in any but the most general rules, the TCPC relies upon the editorial staff to exercise its judgment in making changes in manuscripts, in rearranging and condensing papers, and in making suggestions to authors. The TCPC realizes that the opinions of author and editor may sometimes differ, and hence it is an invariable practice that no paper is published until it has been passed on by the author. For this purpose page proofs of the edited paper are sent to the author prior to publication in a journal. Changes in content and form made in the proofs by authors are followed by the editor except in cases in which the Society's standard spelling and abbreviation forms are affected.

If important differences of opinion arise between author and editor, the points at issue are discussed in correspondence or interview, and if a solution satisfactory to both author and editor is not reached, the matter is laid before the TCPC for adjustment.

AUTHOR QUERY FORM

 ASME <i>SETTING THE STANDARD</i>	Journal: J. Turbomach. Article Number: TURBO-12-1213	Please provide your responses and any corrections by annotating this PDF and uploading it to ASME's eProof website as detailed in the Welcome email.
---	---	---

Dear Author,

Below are the queries associated with your article; please answer all of these queries before sending the proof back to Cenveo. Production and publication of your paper will continue after you return corrections or respond that there are no additional corrections.

Location in article	Query / Remark: click on the Q link to navigate to the appropriate spot in the proof. There, insert your comments as a PDF annotation.
AQ1	In the title and the abstract, please confirm the definition of "UAVs."
AQ2	In the sentence beginning "the current study utilized," please confirm the definition of "CFD."
AQ3	In the sentence beginning "both models were derived," please provide measurement in SI units.
AQ4	In the sentence beginning "selected computationally developed," please provide measurement in SI units.
AQ5	Please review the sentence beginning "Stretched swirling strength" and confirm that the edit made does not change the intended meaning.
AQ6	In the sentence beginning "the pressure side part interacts," please indicate the section being referred to by "the first part of this paper."
AQ7	In the sentence beginning "tip leakage flow," please specify which sections are being referred to by "previous sections."
AQ8	In the sentence beginning "using a combination," please confirm that the correct section has been cited in reference to "the previous section."
AQ9	In the sentence beginning "the tip clearance value," is it correct that Fig. 8 is cited or should it be Fig. 10?
AQ10	In the sentence beginning "A computational model," please indicate which sections are meant by "previous sections."
AQ11	In the sentence beginning "the 22 in," please provide measurement in SI units.
AQ12	In the sentence beginning "in the previous sections," please indicate which sections are meant by "previous sections."
AQ13	In the paragraph beginning "force and torque measurements," please provide all measurements in SI units.
AQ14	In the sentence beginning "since the tip vortex," please indicate which sections are meant by "previous sections."
AQ15	There was no citation for Fig. 19. A citation for Fig. 19 has been inserted. Please confirm that the location of the inserted citation is correct.
AQ16	In the sentence beginning, "the current state-of-the-art," please define "SLA."
AQ17	Please provide page numbers for Ref. 3.
AQ18	Please confirm that all initials in the author list in Ref. 7 are capitalized properly.
AQ19	Please provide page numbers for Ref. 14.
AQ20	Please provide page numbers for Ref. 15.
AQ21	In Ref. 17, please define "AHS."

Thank you for your assistance.

1
2
3
4
5

AQ1

6
8

Ali Akturk¹
e-mail: akturkali@gmail.com

Cengiz Camci²
Professor of Aerospace Engineering
e-mail: cxc11@psu.edu

AQ2
Turbomachinery Aero-Heat Transfer Laboratory,
Department Aerospace Engineering,
Pennsylvania State University,
University Park, PA 16802

Tip Clearance Investigation of a Ducted Fan Used in VTOL Unmanned Aerial Vehicles—Part II: Novel Treatments Via Computational Design and Their Experimental Verification

Ducted fan based vertical lift systems are excellent candidates to be in the group of the next generation vertical lift vehicles, with many potential applications in general aviation and military missions. Although ducted fans provide high performance in many “vertical take-off and landing” (VTOL) applications, there are still unresolved problems associated with these systems. Fan rotor tip leakage flow adversely affects the general aerodynamic performance of ducted fan VTOL unmanned aerial vehicles (UAVs). The current study utilized a three-dimensional Reynolds-averaged Navier-Stokes (RANS) based computational fluid dynamics (CFD) model of ducted fan for the development and design analysis of novel tip treatments. Various tip leakage mitigation schemes were introduced by varying the chordwise location and the width of the extension in the circumferential direction. Reduced tip clearance related flow interactions were essential in improving the energy efficiency and range of ducted fan based vehicles. Full and inclined pressure side tip squealers were also designed. Squealer tips were effective in changing the overall trajectory of the tip vortex to a higher path in radial direction. The interaction of rotor blades and tip vortex was effectively reduced and the aerodynamic performance of the rotor blades was improved. The overall aerodynamic gain was a measurable reduction in leakage mass flow rate. This leakage reduction increased thrust significantly. Experimental measurements indicated that full and inclined pressure side tip squealers increased thrust obtained in hover condition by 9.1% and 9.6%, respectively. A reduction or elimination of the momentum deficit in tip vortices is essential to reduce the adverse performance effects originating from the unsteady and highly turbulent tip leakage flows rotating against a stationary casing. The novel tip treatments developed throughout this study are highly effective in reducing the adverse performance effects of ducted fan systems developed for VTOL UAVs. [DOI: 10.1115/1.4023469]

9 Introduction

10 Ducted fan designs require large tip clearances in order to safely
11 operate in VTOL UAVs. The large tip clearance induced flow has a
12 damaging effect on the fan rotor aerodynamic performance. It is
13 also a significant energy loss mechanism in the ducted fans.

14 This paper describes the development of novel tip treatments
15 for ducted fans used in VTOL UAVs. Ducted fan VTOL UAVs
16 use large tip gaps because of their operating conditions. Large tip
17 clearance flow increases the aerodynamic losses on the fan rotor
18 and diminishes the performance of the ducted fan. Novel tip treat-
19 ments are aimed to reduce the losses and improve performance.

20 There have been a limited number of studies about three-
21 dimensional flow structure of leakage vortex in axial flow fans and
22 compressors in open literature [1–5]. Inoue and Kuromaru et al. [6]

made detailed flow measurements before and behind an axial flow 23
rotor with different tip clearances. In their study, they investigated 24
the clearance effect on the behavior of tip leakage flow. Furukawa 25
and Inoue et al. [7] also investigated breakdown of tip leakage 26
vortex in a low speed axial flow compressor. Reducing tip leakage 27
mass flow rate improves the aerodynamic performance of axial flow 28
fans and compressors. Implementation of treatments in the nonrotat- 29
ing part over the blade tip is also an efficient way of tip leakage 30
flow reduction. References [8] and [9] investigate different casing 31
treatments for axial flow compressors. 32

33 A few authors investigated tip treatments in turbomachinery 34
components for tip leakage mass flow reduction. Corsini et al. 35
[10–14] presented the results of a computational study of an axial 36
flow fan using “improved tip concepts.” The first two end plates 37
were with constant and variable thickness distributions while the 38
last two were designed by combining the end plates with a stepped 39
gap on the tip. The investigation was based on a finite element 40
Navier-Stokes solver for the physical interpretation of the detailed 41
3D leakage flow field. The specific fan performance experiments 42
showed that the improved tip concepts introduced a small perform- 43
ance penalty, but the efficiency curves give evidence of an

¹Currently working in Siemens Energy Inc.

²Corresponding author.

Contributed by International Gas Turbine Institute (IGTI) of ASME for publication in the JOURNAL OF TURBOMACHINERY. Manuscript received November 5, 2012; final manuscript received December 8, 2012; published online xx xx, xxxx. Assoc. Editor: David Wisler.

PROOF COPY [TURBO-12-1213]

44 improvement with better peak performance and a wider high efficiency curve toward the rotor stall margin. An aeroacoustic investigation showed a reduction of the rotor aeroacoustic signature.

45 Wisler [15] presented a study on tip clearance and leakage effects in compressors and fans. He discussed the effect of clearance, duct design, tip treatments, active clearance control, and improving stall margin of rotor blade in his study. He came up with several tip treatment geometries. He tested squealer tip, groove, pressure, and suction side winglet, knife type tip configurations. The most common one of these treatments is the squealer tip obtained by thinning the rotor tip. The main reason for a squealer tip is the reduction of the contact surface during a "rubbing" incidence. A squealer tip has measurable aerodynamic benefits too. Relative to flat tip the deep groove treatment and the pressure surface winglet implementation reduced the leakage.

46 Akturk and Camci [16] developed novel tip platform extensions for energy efficiency gains and aeroacoustic improvements for a constant rotational speed axial flow fan. They measured three components of velocity at downstream of the fan rotor for five different tip platform extensions, introduced on the pressure side of the fan rotor tip section. They showed that the tip platform extensions proved to be effective swirl reducing devices at the exit of the fan. The magnitude of this reduction is about one-third of the rotor exit velocity magnitude in the core of the passage exit. Their results also showed that the mean kinetic energy of fan exit flow increased due to the increase in mean axial velocity.

47 Martin and Boxwell [17] tested two ducted fan models that were designed to effectively eliminate the tip leakage. Both models were derived from the baseline (10-in. inner-diameter shroud), which is explained in their previous study [18]. In their first design, they created a notch and fit the propeller inside the notch. In their second design, a rearward-facing step was cut into the inner shroud. The computational analysis resulted in an increase in inlet lip suction and an increase in performance. However, the experimental thrust and power measurements showed no difference in performance of these designs when compared to their baseline duct.

48 Novel tip platform extensions for aerodynamic and aeromechanic improvements were designed in the current investigation for a ducted fan VTOL UAV in hover condition. Five tip treatments were developed by using numerical solutions of Reynolds-averaged Navier-Stokes equations. Selected computationally developed tip treatments were also experimentally verified in the 22 in. ducted fan test bench. Fan rotor downstream total pressure surveys and force and moment measurements were performed. The main goal of this paper is to develop effective tip treatments for reducing tip leakage flow for large tip gaps used in ducted fans for VTOL UAVs. This paper presents a set of comprehensive ducted fan aerodynamic measurements validating and supporting the computationally developed novel tip treatments named full and partial bump tip extensions, full bump and partial squealer tip extensions, and full squealer and inclined squealer tips in hover condition. A comprehensive assessment and validation of the computational method used in this paper were explained in an accompanying paper by Akturk and Camci [19].

98 Design Algorithm of Tip Treatments

99 **Computational Method.** A three-dimensional computational 100 method can be used to develop novel tip treatments for improving 101 aerodynamic performance of the ducted fan in hover.

102 Reynolds-averaged Navier-Stokes solutions were obtained for 103 computational analysis by using Ansys-CFX. The computational 104 analysis for the tip treatment development was performed on three 105 different computational domains that are connected. The details of 106 the computational method, computational domain sections, grid 107 implementation, and boundary conditions used in this paper can be 108 found in an accompanying paper by Akturk and Camci [19]. The 109 inlet section includes an inlet lip surface that was considered as a 110 solid wall with a no-slip condition. Atmospheric static pressure was

prescribed on the top surface. On the side surface, an opening type 111 boundary condition was assumed. 112

The outlet section includes the outer duct surface, circular rods, 113 rotor hub surface, and support structure underneath of the system 114 that are considered as solid walls with no-slip condition. The bottom 115 surface is also treated with no-slip boundary condition. On the 116 side surface, an opening boundary condition is assumed. 117

The rotating section includes the fan blades, rotor hub region, 118 and shroud surface. The rotating fluid motion at a constant angular 119 velocity is simulated by adding source terms to the Navier-Stokes 120 equations for the effects of the Coriolis force and the centrifugal 121 force. Counterrotating wall velocities are assigned at the shroud 122 surface. 123

124 Stationary and rotating regions were subsectional by periodic 125 surfaces. By the help of periodicity, the speed of numerical simulations 126 was increased. The stationary surfaces were divided into four 127 segments, and the rotating region was divided into eight periodic 128 segments. Only one of these segments for each region was used in 129 numerical calculations. The difference in pitch angles of the frames 130 was taken into account in interfaces that are connecting rotating 131 and stationary surfaces. A stage type interface model was used. 131

132 The stage model performs a circumferential averaging of the 133 fluxes on the interface surface. This model allows steady state predictions 134 to be obtained for turbomachinery components. The stage 135 averaging at the frame change interface introduces one-time 136 mixing loss. This loss is equal to assuming the physical mixing 137 supplied by the relative motion between stationary and rotating 138 surfaces. General grid interface (GGI) was used for mesh connections 139 between interfaces.

140 Figure 1 illustrates a view from medium size computational 141 mesh near the squealer and inclined squealer rotor tips. Nondimensional 142 wall distance (y^+) less than 2 was achieved near the 143 shroud, rotor tip, and treatment surfaces.

144 The numerical simulations for tip treatments were obtained at 2400 rpm rotor speed for hover condition. Calculations were performed using a parallel processing approach. For the parallel processing, the stationary and rotating frames were partitioned via 147 vertex based partitioning with METIS multilevel k-way algorithm. 148 Computations were performed on a cluster having 24 processors. 149 Total processing time was approximately 54.9 h. The flow within 150

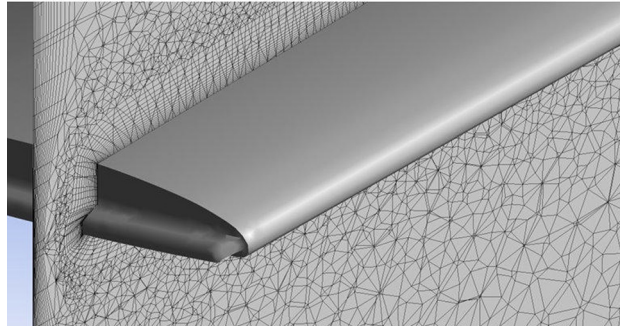
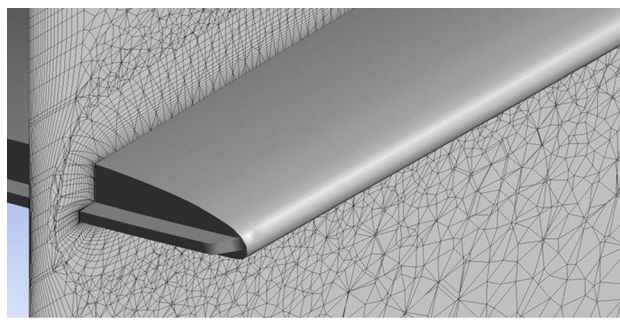


Fig. 1 The near tip computational grid for squealer and inclined squealer rotor tips

PROOF COPY [TURBO-12-1213]

151 the computational domain was initialized as no flow at the free-
 152 stream static conditions. The convergence solution was achieved
 153 approximately within 4500 iterations. The root mean square (rms)
 154 residuals of the Navier–Stokes equations were compared for judging
 155 convergence.

156 **Blade Tip Constant Circumferential Angle Planes.** The visualiza-
 157 tion planes obtained at constant circumferential angles were
 158 generated at the rotor blade tip for a better understanding of the
 159 rotor tip region flow. They were all passing from the axis of rotation
 160 and drawn at fixed circumferential position (θ). Three of these
 161 planes (A, B, and C) were drawn just upstream of the rotor tip and
 162 they were separated by 4 deg circumferential angle from each
 163 other and plane D. Plane D was drawn at the quarter chord of the
 164 tip profile. Planes E, F, G, H, and I were equally distributed
 165 near the rotor tip profile by 2 deg circumferential angle incre-
 166 ments. Plane I was drawn at the trailing edge.

167 Constant circumferential angle planes drawn in Fig. 2 are col-
 168 orded with the magnitude of stretched swirling strength. Swirling
 169 strength is the imaginary part of complex eigenvalues of velocity
 170 gradient tensor. It is positive if and only if there is existence of a
 171 swirling local flow pattern and its value represents the strength of
 172 swirling motion around local centers. Stretched swirling strength
 173 is swirling strength times the product of swirling vector and nor-
 174 mal of swirling plane. An increase in this parameter indicates that
 175 swirling strength normal to swirling plane is increased.

176 The quantity color coded in these planes is the velocity
 177 stretched swirling strength drawn on the constant circumferential
 178 angle planes. The swirling strength shows the magnitude of the
 179 out of plane swirling motion. The red color indicates a region that
 180 the highest swirling motion is occurring. Planes A, B, and C show
 181 swirling strength upstream of the rotor blade. A small amount of
 182 swirling motion can be observed in these planes that is related to
 183 the tip vortex originating from the previous blade. The positioning
 184 of each tip vortex influencing the neighboring blade is clearly
 185 shown in Part I of this paper [19]. The vortical field originating
 186 from the previous blade tip vortex interacts with the blade tip.
 187 This vortical field is divided into two parts as suction side and
 188 pressure side parts. The suction side part is integral with the tip
 189 vortex of the current blade. The pressure side part interacts with
 190 the pressure side of the rotor blade and generates additional loss at
 191 the exit plane that is shown in the first part of this paper. The
 192 strongest swirling motion starts at the quarter chord of the blade
 193 tip measured from the leading edge. Leakage flow tries to pass to
 194 the suction side by generating a vortical structure that is visible at
 195 plane D. In planes E, F, G, H, and I the path of the released vortic-
 196 al structure from the pressure side corner can be viewed. Once
 197 the vortical structure forms, the strength of it is not as high as the

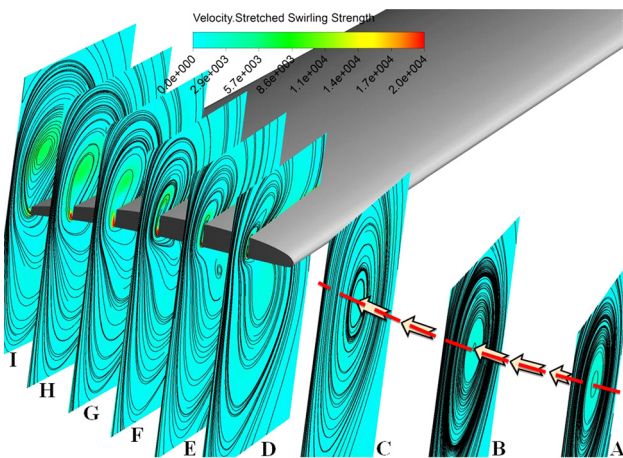


Fig. 2 Blade tip constant circumferential angle planes drawn for baseline rotor tip with 3.04% tip clearance

198 one observed near the pressure side corner seen in plane D. The
 199 size of the flow structure dominated by light blue and green zones
 200 is increasing when one travels from the leading edge to trailing
 201 edge.

Tip Treatment Geometries

202

AQ7

203 Tip leakage flow results in a considerable amount of aerody-
 204 namic loss in rotor flow field as discussed in previous sections.
 205 One way of reducing tip losses is to use proper tip treatments. The
 206 specific tip treatments subject to investigation in this paper
 207 include special extensions of rotor tip platform and squealer tips.
 208 Both types of tip treatments are widely used in axial flow fans and
 209 compressors. Figure 3 shows the tip platform extension concepts
 210 and squealer tip concepts that are subject to investigation in this
 211 section.

212 **Partial Bump Tip Platform Extension.** Effectiveness of par-
 213 tially blocking the pressure side of the fan rotor tip in mitigating
 214 tip leakage was explained by Akturk and Camci [16]. It was
 215 shown that profiles 1 and 2 that are using partial bump type tip
 216 platform extension at the pressure side of the fan rotor tip were
 217 the best choices for reducing the effects of tip leakage and
 218 improving axial flow velocity at the rotor downstream for the
 219 lightly loaded fan rotor. Those two bump profiles had the same
 220 thickness with the rotor tip profile at the bump center location.
 221 The bump thickness was measured in the circumferential plane at
 222 a constant radial position.

223 The partial bump designed for the current VTOL UAV ducted
 224 fan shares the same idea: *reducing the tip leakage flow originating*
from the pressure side corner of the blade tip. Computational
 225 investigations for the baseline fan rotor with 3.04% tip clearance
 226 discussed in Part I of this paper showed that the tip leakage starts
 227

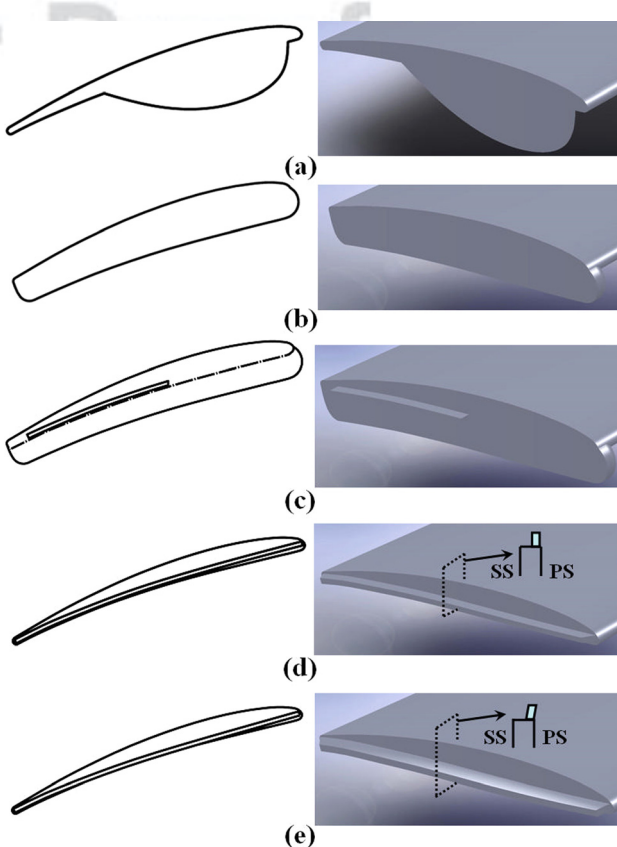


Fig. 3 Tip treatments (a) Partial bump tip platform extension (t.p.e.), (b) full bump t.p.e., (c) full bump and partial squealer t.p.e., (d) full squealer t.p.e., (e) Inclined full squealer t.p.e

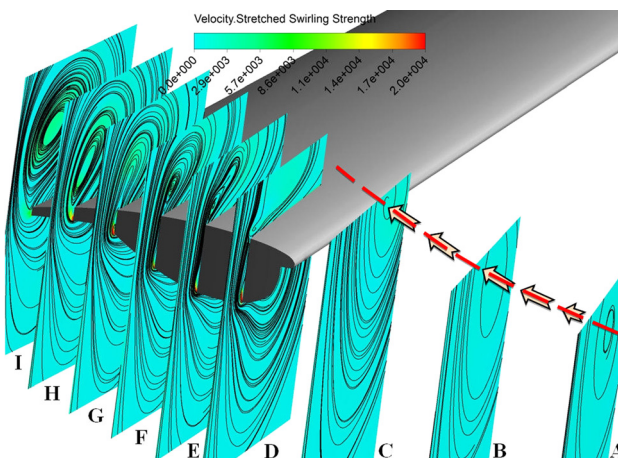


Fig. 4 Blade tip constant circumferential angle planes drawn for “partial bump” tip extension with 3.04% tip clearance

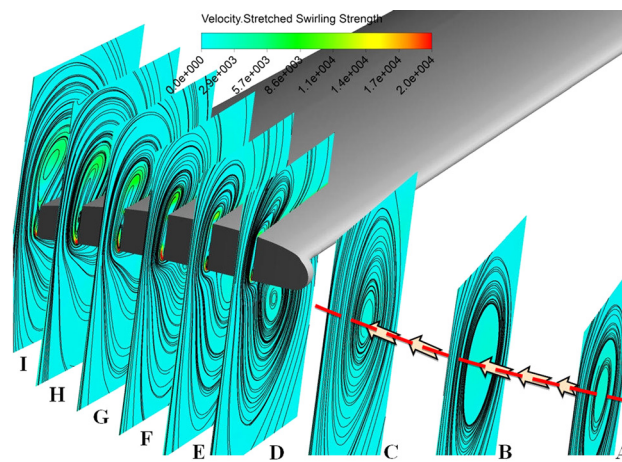


Fig. 5 Blade tip constant circumferential angle planes drawn for “full bump” tip extension with 3.04% tip clearance

very close to the leading edge of the tip profile. Therefore, a long bump starting from the 5% of chord location and ending at 66.6% tip chord location was designed. The maximum thickness point was selected as the quarter chord (25% of the tip chord) since the highest swirling strength was observed in that location. The maximum thickness of the bump was chosen as “twice the tip chord thickness” at the quarter chord location. Figure 3(a) shows the shape of the bump designed.

Figure 4 shows streamlines and stretched swirling strength contour for partial bump tip extension shown in Fig. 3(a). Planes A, B, and C show tip vortex coming from the previous blade moving radially inward compared to the baseline tip result. The strongest contribution to tip vortex is near plane G. However, a gradual increase in the swirling strength is observed in planes D, E, and F. Tip vortex can be seen in planes G, H, and I with a light green and blue core. The strength of the vortex is slightly higher than the ones obtained for the baseline tip.

Full Bump Tip Platform Extension. Since the leakage flow cannot be effectively blocked by using partial bump tip extension, a full coverage bump tip platform extension was designed to cover the pressure side of the rotor tip completely. The bump starting from the leading edge and ending at the trailing edge of the tip chord was designed. Bump was created by extending pressure side curvature by the airfoil thickness at the quarter chord point of the blade profile. Figure 3(b) shows the shape of the full bump designed.

Figure 5 shows the streamlines and stretched swirling strength contour for full bump tip extension. Planes A, B, and C show tip vortex coming from the previous blade moved more axially compared to the baseline tip and the partial bump result. Full bump tip extension was not sufficient for effectively reducing the leakage flow. Planes D, E, F, G, H, and I show that the strength of the vortical structure was almost same with the baseline rotor tip without a beneficial tip mitigation influence.

Full Bump and Partial Squealer Tip Platform Extension. Since the leakage flow cannot be properly blocked by using only pressure side tip extensions, a combination of a full bump and a partial squealer extension was designed for the region near the trailing edge. Figure 3(c) shows the shape of the combined full bump and partial squealer design. The squealer extension started from 45% chord measured from leading edge and ended at the trailing edge. The height of the squealer was 0.89 mm and thickness was 20% of the tip gap height (1.27 mm for 3.04% tip clearance). The squealer tip was located parallel to the pressure side of the rotor tip and approximately 0.5 mm away from the pressure side.

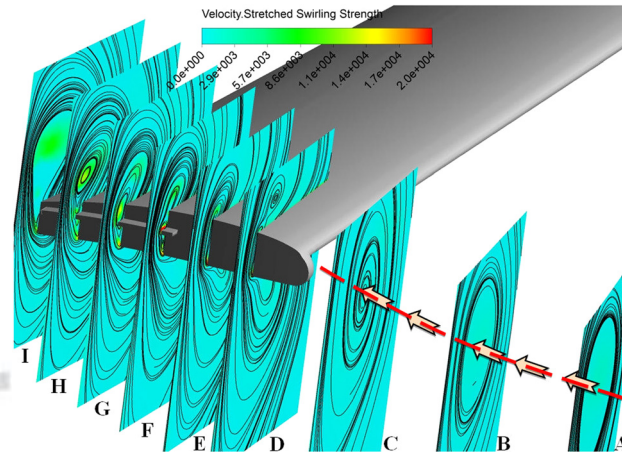


Fig. 6 Blade tip constant circumferential angle planes drawn for “full bump and partial squealer” tip extension with 3.04% tip clearance

Figure 6 shows streamlines and stretched swirling strength contour for a combination of the full bump and squealer tip extension. Planes A, B, and C show tip vortex coming from the previous blade moving more axially compared to baseline tip and partial bump result. Full bump and squealer tip extension were not sufficient for blocking leakage flow. Planes F, G, H, and I show the effect of squealer on the flow field near the rotor tip. By the effect of the squealer the swirling strength was increased and tip vortex was moved radially outward, which is a favorable effect. Moving the tip vortex radially out will reduce the interactions between the tip vortex and rotor blade and reduce the losses. However, the combination of full bump and partial squealer increased swirling strength and losses.

Full Squealer Tip Platform Extension. Using a combination of bump and squealer increased turbulence and swirl at the rotor tip as shown in Full Bump and Partial Squealer Tip Platform Extension. A full squealer tip extension was designed to explore its potential as a possible aerodynamic tip mitigation device. Figure 3(d) shows the shape of the full squealer tip designed for this. Squealer extension started from the leading edge of the rotor tip and ended at the trailing edge. The width of the squealer was 0.89 mm and height was 20% of the tip gap height (1.27 mm for 3.04% tip clearance). The squealer tip was located parallel to the pressure side of the rotor tip and 0.5 mm away from pressure side. At the leading edge of the

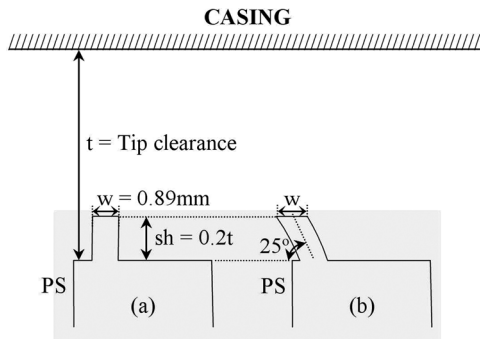


Fig. 7 (a) Full and (b) inclined squealer sketch

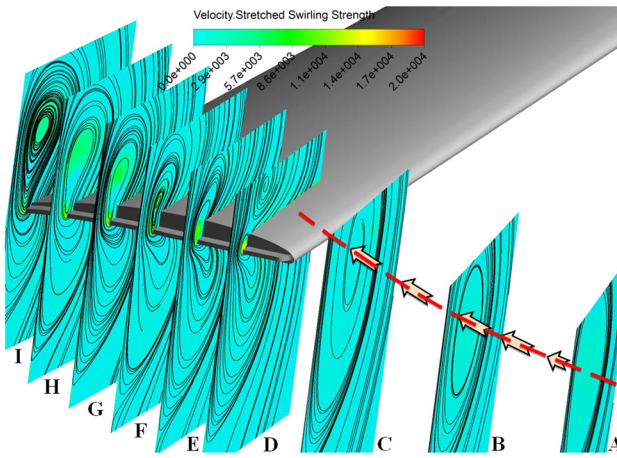


Fig. 8 Blade tip constant circumferential angle planes drawn for "full squealer" tip extension with 3.04% tip clearance

tip profile, it was aligned with the stagnation point of the tip profile. Figure 7 shows a sketch of full and inclined squealers.

Figure 8 shows streamlines and stretched swirling strength contour for full squealer tip extension. Squealer tip extension decreased the strength of swirling at planes D, E, F, G, H, and I. The leakage flow starting from the pressure side rolled up a small vortical structure between the squealer and suction side. After plane F, the vortical structure appeared on the suction side of the rotor tip. Tip vortex started to influence the passage flow beginning plane F. Using a squealer tip also moved tip vortex closer to the shroud and relieved the rotor passage from the adverse effect of tip vortex dominated flow. Thus, interaction of tip vortex and rotor tip was reduced and the rotor tip was loaded better than the baseline rotor tip because of improvements in the passage aerodynamics near the tip.

Inclined Full Squealer Tip Platform Extension. Using the full squealer tip design moved tip vortex toward the shroud. The most important effect of the squealer tip was delaying tip vortex at the rotor tip. The leakage flow was filled into the space between the squealer and suction side of the rotor blade and released on the suction side at the midchord location. Delaying tip vortex release to a chordwise location close to the trailing edge helped to direct tip vortex radially out. Further improvement can be obtained by increasing space between the squealer and suction side of the rotor tip by bending squealer extension toward to pressure side. A fully inclined squealer tip extension was designed by tilting the existing squealer extension about 25 deg toward the pressure side. This inline squealer design is shown in Figs. 7 and 3(e).

Figure 9 shows streamlines and stretched swirling strength contour for inclined squealer tip extension. The leakage flow originat-

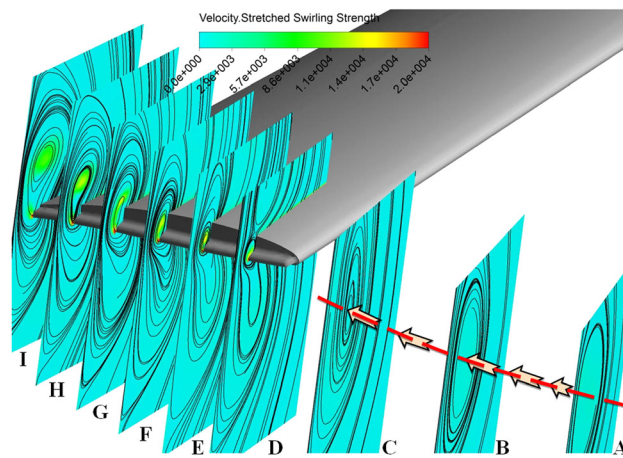


Fig. 9 Blade tip constant circumferential angle planes drawn for "inclined squealer" tip extension with 3.04% tip clearance

ing from the pressure side rolled up a small vortical structure between the inclined squealer and suction side. After plane G, the vortical structure appears near the suction side of the rotor tip. Tip leakage vortex originates starting from plane G and was directed toward the shroud region.

Overall Benefits of Tip Treatments

Overall benefits gained from the tip treatments are analyzed by total pressure improvements in the stationary frame of reference. Table 1 shows computed thrust and ratio of "leakage mass flow rate" to the "fan rotor mass flow rate" for baseline rotor tips for two tip clearances and treated tips. The leakage mass flow rate was calculated on a plane that was defined between the rotor tip and shroud surface.

The result from the two tip clearances, tight (1.71%) and coarse (3.04%), are compared in Table 1. When the tip clearance decreased, the leakage mass flow rate also decreased and thrust was augmented. Decrease in leakage mass flow rate usually implies an increase of overall mass flow rate passing from the duct.

The first two rows of Table 1 present a comparison of both experimental and computational values of ducted fan thrust. The computational thrust results and measured values compare very well at two specific tip clearance values at 1.71% and 3.04%. All of the tip treatments shown in Table 1 are computationally evaluated at the same tip clearance of 3.04%. Aeromechanic and aerodynamic performance improvements provided by tip treatments are also tabulated in Table 1.

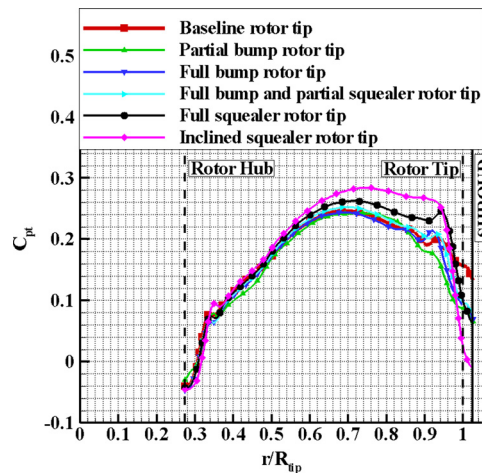
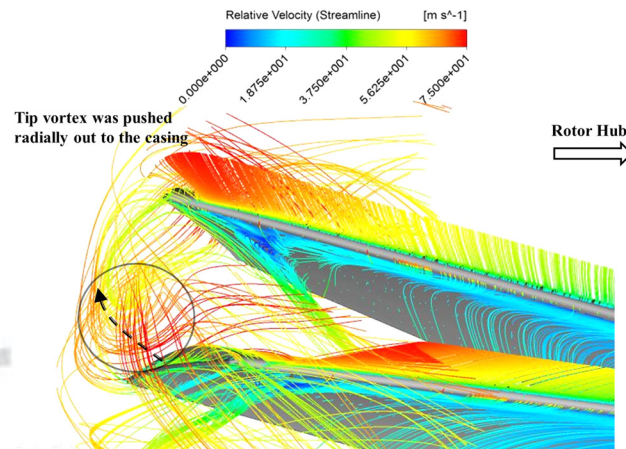
Figure 10 compares all of the tip treatments by comparing the spanwise total pressure distributions in the stationary frame of reference. The computationally obtained total pressure distributions are drawn at the same rotor exit plane in which the baseline measurements are performed. This plane is located at about 45.72 mm downstream from the midspan of the fan rotor. The tip clearance value for all computations presented in Fig. 8 is 3.04%.

Because of the increased viscous losses induced at the rotor tip and radial tip leakage flow directed spanwise inward, the performance of partial and full tip platform extensions was lower than the baseline profile. Thrust obtained from the ducted fan was reduced for both treatments. Full tip platform extension combined with a partial squealer effectively reduced the tip leakage flow compared to partial and full tip platform extensions. However, those gains provided by this treatment were not as high as the squealer tip treatments. Full squealer and inclined full squealers were the best performing ones. They improved the aerodynamic performance by moving the tip vortex toward the shroud. The inclined squealer tip increased the thrust provided by the ducted fan by 10.73% at

AQ9

Table 1 Tip treatments and their computed performance in hover condition at 2400 rpm

Ducted fan performance with baseline fan rotor tip				
	$\frac{\dot{m}_{\text{leakage}}}{\dot{m}_{\text{fan}}} (\%)$	Total thrust (N)(comp.)	Total thrust (N) (exp.)	$\epsilon(\%)$
Baseline rotor tip with 1.71% t. c.	1.81	94.24	92.68	1.68
Baseline rotor tip with 3.04% t. c.	3.41	85.16	83.55	1.93
Baseline rotor tip with 5.17% t. c.	6.35	61.96	67.55	8.27
Ducted fan performance using treated fan rotor tips with 3.04% tip clearance (computational only)				
	$\frac{\dot{m}_{\text{leakage}}}{\dot{m}_{\text{fan}}} (\%)$	D. thrust (N)	R. thrust (N)	Total thrust (N)
Baseline rotor tip	3.41	27.20	57.96	85.16
Partial bump t.p.e.	3.58	26.68	54.06	80.74
Full bump t.p.e.	3.28	26.70	58.20	84.90
Full bump and par. squealer t.p.e.	2.86	27.66	58.68	86.34
Full squealer t.p.e.	2.41	30.50	59.81	90.31
Full inclined squealer t.p.e.	2.35	30.76	63.55	94.31

**Fig. 10 Comparison of computationally obtained total pressure distributions for all of the tip treatments and baseline rotor tip (3.04% tip clearance)****Fig. 11 Streamlines around the inclined squealer rotor blade with 3.04% tip clearance and rotor hub at 2400 rpm**

374 the hover condition 2400 rpm. It also decreased tip leakage mass
375 flow rate at a considerable rate as shown in Table 1.

376 Figure 11 shows the streamlines drawn around the tip and mid-
377 span regions for the fan rotor blade with inclined squealer tips.
378 Streamlines are colored by relative velocity magnitude and drawn
379 in the relative frame of reference. The inclined squealer tip
380 directed tip leakage jet toward the casing area as shown in Fig. 11.
381 As a result, the relative velocity magnitudes near the tip region
382 and midspan were increased due to less interaction of leakage jet
383 with the pressure side of the neighboring blade.

384 Experimental Verification of Computationally 385 Developed Tip Concepts

386 **Experimental Approach.** The current study concentrates on
387 the rotor tip section aerodynamic performance improvement by
388 developing novel tip treatments. A computational model was used
389 in the design and analysis of tip treatments as outlined in the pre-
390 vious sections. Selected treatments were tested using experimental
391 methods. Experimental methods used for this research were total
392 pressure survey at rotor exit and aeromechanic measurements of
393 the ducted fan system.

394 Fan rotor exit total pressure measurements in the stationary
395 frame of reference were performed by using a Kiel total pressure

probe. The Kiel total pressure probe having a 5 mm diameter total head was traversed in radial direction using a precision linear traverse mechanism controlled by a computer. The total pressure probe was always located 45.72 mm downstream of the fan rotor exit plane at 50% of blade span (midspan). The Kiel probe was aligned with absolute rotor exit velocity at midspan position. Details of the probe alignment for different spanwise positions are explained in detail in Part I of this paper [19].

396 Ducted fan aerodynamic research performed in this study 397 requires high accuracy force and moment measurements. The 22 398 in. diameter fan was equipped with an ATI-Delta six component 399 force and torque transducer. Three components of force and three 400 components of moments were measured. Part I of this paper 401 explains the details of the force and torque measurement details 402 and uncertainties.

403 **Manufacturing Tip Platform Extensions Using a Stereolithography Based Rapid Prototyping Technique.** In the previous 404 sections, the computational analysis was performed for 405 selecting the best tip profile geometries for improving aeromechanic 406 and aerodynamic performance of the system. Squealer and 407 inclined squealer tips both improved thrust of the system while 408 reducing leakage mass flow rate. They also improved fan rotor 409 exit total pressure distribution compared to baseline rotor tips. 410 Three different squealer and inclined squealer designs were 411 selected to be manufactured and experimentally tested in hover 412 413 414 415 416 417 418 419 420

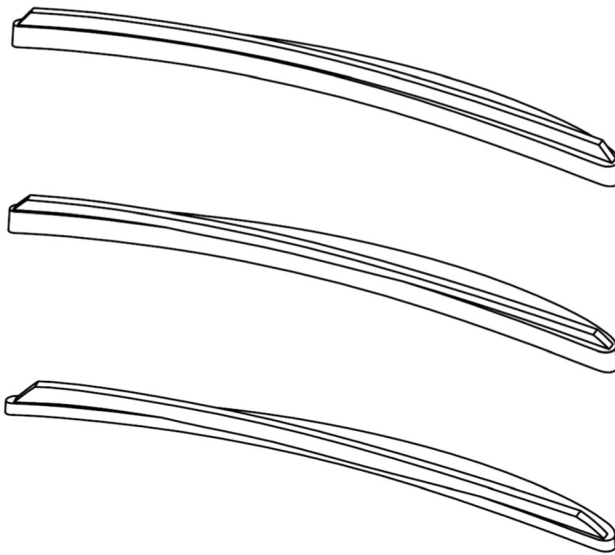
PROOF COPY [TURBO-12-1213]

Fig. 12 Squealer and inclined squealer tip extensions designed for SLA manufacturing (a) squealer t.p.e.(3.04% t.c.), (b) inclined squealer t.p.e.(3.04% t.c.), (c) inclined squealer t.p.e.(5.17% t.c.)

421 condition. The baseline tip clearance level for the computational
422 analysis was 3.04%. For the experimental program, squealer and
423 inclined squealer tip treatments were designed for 3.04%. Inclined
424 squealer tip treatment was also tested for 5.17% tip clearance.

425 Selected tip shapes were designed as an extension to the tip of a
426 baseline fan rotor tip. These extensions conformed to the external
427 contour of the baseline tip section. Figure 12 shows drawings of
428 the extensions designed for the baseline fan rotor tips. The exten-
429 sions were glued to the top surface of the fan rotor blade using
430 cyanoacrylate that had high viscosity and high impact strength.
431 Figure 13 shows a rotor blade tip that has an inclined squealer tip
432 extension attached to it. Each tip concept tested had its own eight
433 bladed rotor assembly. The tip clearance was measured from the
434 base of the attached tip concept model as shown in Fig. 13.

435 Experimental Results

AQ13 **436 Force and Torque Measurements.** Force and torque measure-
437 ments for fan rotors with treated tips were performed in the 22 in.
438 diameter axial flow fan research facility described in Part I of this
439 paper. Figure 14 shows measured thrust coefficient at various rota-
440 tional speeds. The squealer and inclined tip squealer tip shapes
441 were both augmenting thrust of the system compared to baseline
442 rotor tip shapes. A maximum increase of 9.1% was gained by
443 using the squealer tip shape at 2700 rpm. The maximum increase
444 in thrust gained by using an inclined squealer tip was around 9.6%
445 at 2700 rpm. Compared to computational results, experimental
446 performance of squealer tips was better than computational per-
447 formance in terms of measured thrust values. Using tip treatments

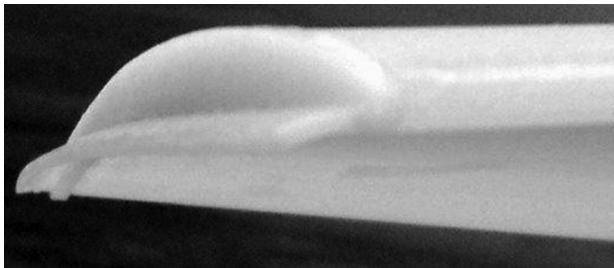


Fig. 13 Inclined squealer t.p.e. applied to the rotor blade (5.17% tip clearance)

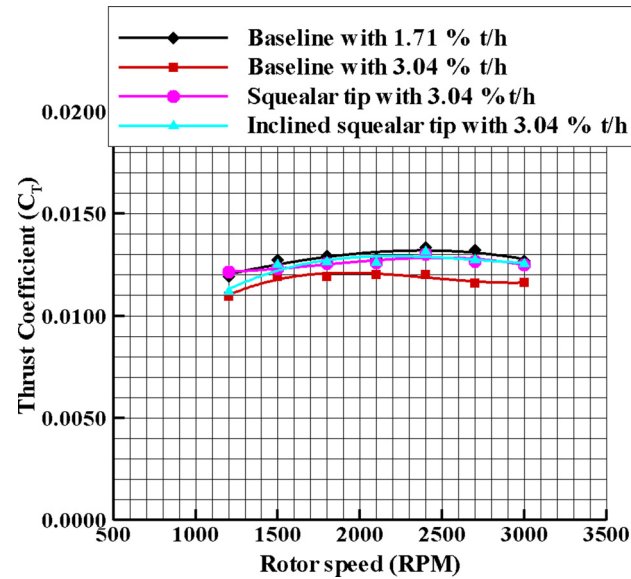


Fig. 14 Measurements of thrust coefficient versus rotational speed for the rotor with squealer and inclined squealer tips at 3.04% tip clearance

improved performance of the baseline rotor tips with 3.04% tip clearance such that the fan rotor with treated tips at the same tip clearance (3.04%) performed almost as well as the baseline fan rotor performance having a tighter tip clearance (1.71%), without any tip treatment. These comparisons are based on measured thrust in the 22 in. diameter ducted fan research facility. The height of the squealer tips used in this study was always one-fifth of the effective clearance t measured between the casing surface and the base platform of the blade tip.

Figure 15 illustrates the aeromechanic performance of an inclined squealer at 5.17% tip clearance compared to baseline rotor at the same clearance. When treatments were used with larger clearance, the improvements obtained were better. Total improvement in thrust was 15.9% at 2700 rpm. Performance of the baseline rotor tips at 5.17% tip clearance was enhanced so that

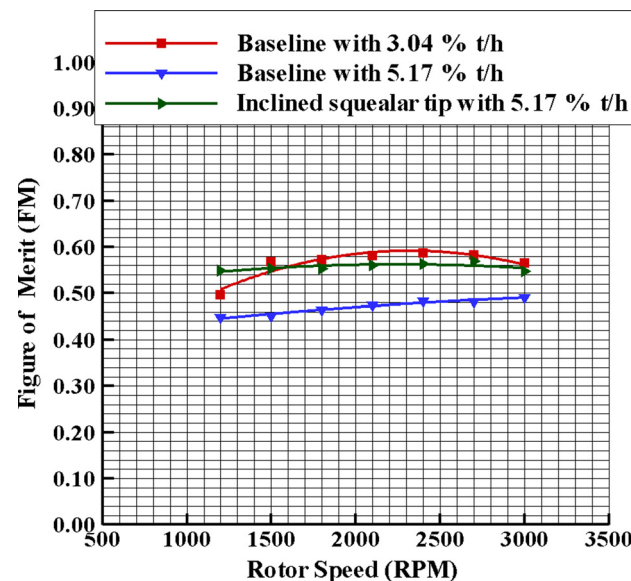


Fig. 15 Measurements of thrust coefficient versus rotational speed for rotor with squealer and inclined squealer tips at 5.17% tip clearance

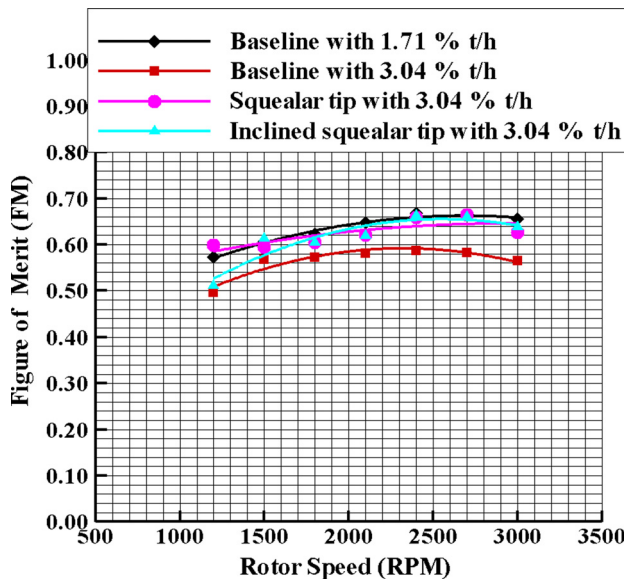


Fig. 16 Measured figure of merit versus rotational speed for rotor with squealer and inclined squealer tips at 3.04% tip clearance

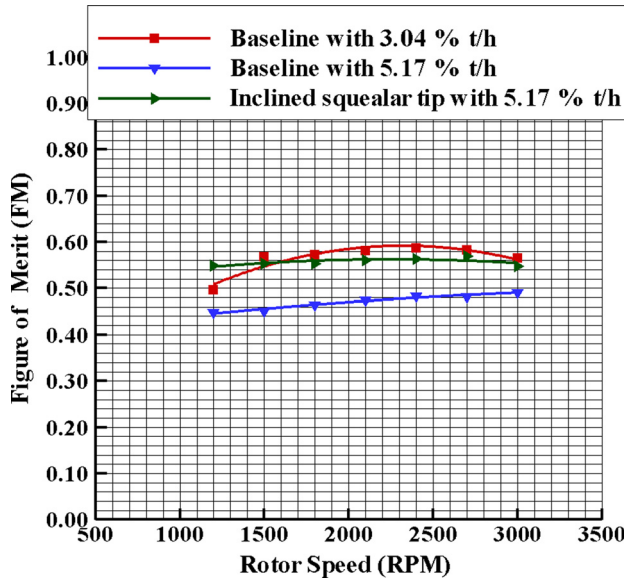


Fig. 17 Measured figure of merit versus rotational speed for rotor with squealer and inclined squealer tips at 5.17% tip clearance

they are almost performing like the 3.04% tip clearance baseline rotor, without any tip treatment.

Figures 16 and 17 illustrate the measured figures of merit plotted against the rotational speed of the fan rotor. Squealer and inclined squealer rotor tips increased hover efficiency compared to baseline rotor tips. Treated tip shapes at 5.17% tip clearance performed better than 3.04% tip clearance (no tip treatments).

Total Pressure Measurements. Aerodynamic performance of the ducted fan with squealer rotor tips was assessed by fan rotor exit total pressure measurements at hover condition. Figure 18 shows total pressure coefficient measured at fan rotor downstream from rotor hub to the shroud. It should be noted that there was almost no change in total pressure coefficient by using treated tips when $r/R_{tip} \leq 0.35$. Total pressure at the fan rotor exit plane was increased by using squealer and inclined squealer tip designs at

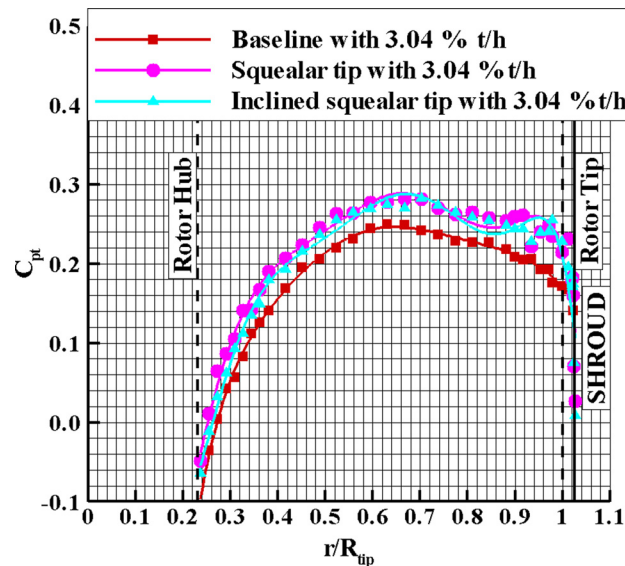


Fig. 18 Total pressure measured at downstream of the rotor at 2400 rpm for squealer tips with 3.04% tip clearance

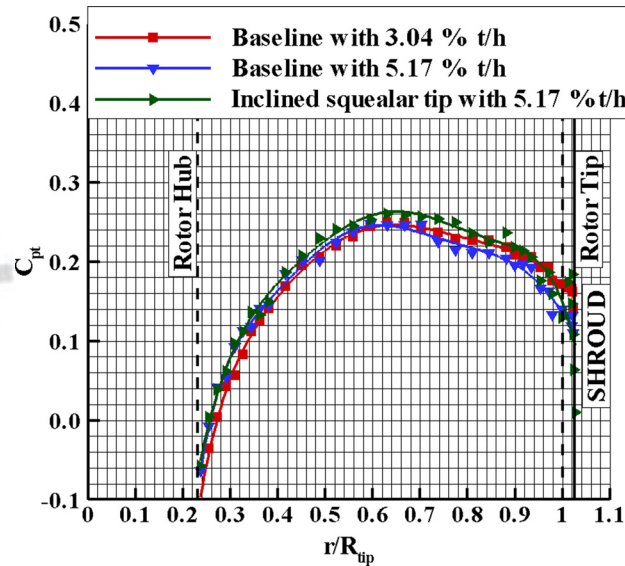


Fig. 19 Total pressure measured at downstream of the rotor at 2400 rpm for squealer tips with 5.17% tip clearance

3.04% tip clearance. Since the tip vortex that is originating from the rotor tip pressure side is repositioned by squealer and inclined squealer tips as mentioned in previous sections, total pressure distribution at the rotor tip where $r/R_{tip} \geq 0.3$ was enhanced. A significant portion of the blade span above $r/R_{tip} \geq 0.3$ produced a measurably higher total pressure as shown in Fig. 18. The total pressure augmentation from the tip treatments were particularly effective near the blade tip where $r/R_{tip} \geq 0.85$. For the larger tip clearance 5.17% (Fig. 19), using an inclined squealer tip also improved the total pressure distribution near the rotor tip region and performed better than the smaller tip clearance baseline tip performance at 3.04%.

Conclusions

This paper presents a set of comprehensive ducted fan aerodynamic measurements validating and supporting the computationally developed novel tip treatments. The new tip treatments are referred as full and partial bump tip extensions, full bump and

495 partial squealer tip extensions, and full squealer and inclined
496 squealer tips.

497 The losses generated were highly related to the tip vortex trav-
498 eling direction and trajectory. If the tip vortex traveled radially
499 inward, then the losses related to the blockage effect influenced a
500 larger portion of the blade span and the rotor tip stall was more
501 pronounced.

502 The current study used squealer heights that had a total height
503 of one-fifth of the effective clearance t between the base platform
504 and the casing. A full squealer rotor tip was effective in changing
505 the direction of the tip vortex. The tip vortex was pushed radially
506 out to the casing area. The computational results showed that the
507 squealer tip successfully blocked the tip vortex between leading
508 edge and midchord of the rotor tip profile.

509 An inclined full squealer tip was also conceived to move tip
510 vortex origination location closer to the trailing edge. This was
511 achieved by allocating more space to the tip vortex to fill between
512 squealer and suction side of the rotor tip.

513 Overall aeromechanic performance gains obtained by using tip
514 platform extensions were assessed from computations. Pres-
515 sure side tip platform extensions reduced thrust obtained from the
516 ducted fan.

517 The best performing profiles were full and inclined full squealer
518 extensions. Both experimental measurements and computations
519 confirmed this observation. Full squealer tip extension increased
520 thrust of the ducted fan by 6.04% and reduced the leakage mass
521 flow rated by 29.3% compared to the baseline rotor tips. Inclined
522 squealer tips increased the thrust by 10.73% while reducing the
523 leakage mass flow rate by 31.0%.

524 Experimental investigation was also performed by manufacturing
525 squealer and inclined squealer tip extensions for 3.04% tip
526 clearance and inclined squealer tip extensions for 5.17% tip clear-
527 ance. Solid models of tip extension pieces originally developed
528 for computational purposes were directly used to manufacture ex-
529 perimental tip treatment models in a rapid prototyping process.

530 Aeromechanic and aerothermodynamic measurements showed
531 that using full inclined squealer tips with 5.17% tip clearance is
532 equivalent to working with a 3.04 tip clearance baseline rotor.

533 The squealer and inclined squealer tips at 3.04% tip clearance
534 also improved performance of the fan rotor. This operation was
535 equivalent to working with a baseline rotor at 1.71% tip clearance.
536 This feature of the tip treatments allows using treated rotor blades
537 at larger clearances while performing as well as operating at much
538 smaller clearances.

539 The novel tip treatments filling one-fifth of the effective gap
540 between the tip platform and the casing can easily be manufac-
541 tured out of attachable and flexible materials for VTOL UAV fan
542 implementation. The current state-of-the-art in SLA manufac-
543 turing allows the rapid production of the proposed tip treatments out
544 of materials such as rubber or other flexible plastic materials of
545 resilient character.

546 While the flexible tip treatments improve ducted fan thrust and
547 reduce tip clearance leakage mass flow rate, they can be quickly
548 replaced in case of a rubbing incident during field operation.

Acknowledgment

549 The authors acknowledge the financial support provided by The
550 Pennsylvania State University Vertical Lift Center of Excellence
551 (VLRCOE) and National Rotorcraft Technology Center (NRTC)
552 (Under U.S. Army Research Office Grant No. W911W6-06-2-
553 0008). They wish to thank Ozhan Turgut for his support throughout
554 this effort. They are also indebted to Mr. Harry Houtz for his tech-
555 nical support.

References

- [1] Lee, G. H., Baek, J. H., and Myung, H. J., 2003, "Structure of Tip Leakage in a Forward-Swept Axial-Flow Fan," *Flow Turbul. Combust.*, **70**, pp. 241–265. 557
- [2] Jang, C. M., Furukawa, M., and Inoue, M., 2001, "Analysis of Vortical Flow Field in a Propeller Fan by LDV Measurements and LES—Parts I, II," *ASME J. Fluid. Eng.*, **123**, pp. 748–761. 558
- [3] Storer, J. A., and Cumpsty, N. A., 1991, "Tip Leakage Flow in Axial Compressors," *ASME J. Turbomach.*, **113**. 559
- [4] Lakshminarayana, B., Zaccaria, M., and Marathe, B., 1995, "The Structure of Tip Clearance Flow in Axial Flow Compressors," *ASME J. Turbomach.*, **117**, pp. 336–347. 560 AQ17
- [5] Matzgeller, R., Bur, P., and Kawall, J., 2010, "Investigation of Compressor Tip Clearance Flow Structure," *Proceedings of ASME Turbo Expo 2010: Power for Land, Sea and Air*, GT2010-23244. 561
- [6] Inoue, M., Kuroamaru, M., and Furukawa, M., 1986, "Behavior of Tip Leakage Flow Behind an Axial Compressor Rotor," *ASME J. Gas Turb. Power*, **108**, pp. 7–14. 562
- [7] Furukawa, M., Inoue, M., Kuroamaru, M., Saik, i. K., and Yamada, K., 1999, "The Role of Tip Leakage Vortex Breakdown in Compressor Rotor Aerodynamics," *ASME J. Turbomach.*, **121**, pp. 469–480. 563
- [8] Fujita, H., and Takata, H., 1984, "A Study on Configurations of Casing Treatment for Axial Flow Compressors," *B. JSME*, **27**, pp. 1675–1681. 564
- [9] Moore, R. D., Kovich, G., and Blade, R. J., 1971, "Effect of Casing Treatment on Overall and Blade-Element Performance of a Compressor Rotor," NASA, Tech. Rep. TN-D6538. 565
- [10] Corsini, A., Perugini, B., Rispoli, F., Kinghorn, I., and Sheard, A. G., 2006, "Investigation on Improved Blade Tip Concept," *ASME Paper GT2006-90592*. 566
- [11] Corsini, A., Rispoli, F., and Sheard, A. G., 2006, "Development of Improved Blade Tip End-Plate Concepts for Low-Noise Operation in Industrial Fans," *Proceedings of Conference on Modeling Fluid Flows CMMF06*. 567
- [12] Corsini, A., Perugini, B., Rispoli, F., Kinghorn, I., and Sheard, A. G., 2007, "Experimental and Numerical Investigations on Passive Devices for Tip-Clearance Induced Noise Reduction in Axial Flow Fans," *Proceedings of the 7th European Conference on Turbomachinery*. 568
- [13] Corsini, A., Perugini, B., Rispoli, F., Sheard, A. G., and Kinghorn, I., 2007, "Aerodynamic Workings of Blade Tip End-Plates Designed for Low-Noise Operation in Axial Flow Fans," *ASME Paper GT2007-27465*. 569
- [14] Alessandro, C., Franco, R., and Sheard, A. G., 2010, "Shaping of Tip End-Plate to Control Leakage Vortex Swirl in Axial Flow Fans," *ASME J. Turbomach.*, **132**(3). 570
- [15] Wisler, D., 1985, "Tip Clearance Effects in Axial Turbomachines," Von Karman Institute for UID Dynamics Lecture Series, (5). 571
- [16] Akturk, A., and Camci, C., 2010, "Axial Flow Fan Tip Leakage Flow Control Using Tip Platform Extensions," *ASME J. Fluids Eng.*, **132**(5). 572
- [17] Martin, P. B., and Boxwell, D. A., 2005, "Design, Analysis and Experiments on a 10-Inch Ducted Rotor VTOL UAV," *AHS International Specialists Meeting on Unmanned Rotorcraft: Design, Control and Testing*. 573
- [18] Martin, P., and Tung, C., 2004, "Performance and Flowfield Measurements on a 10-Inch Ducted Rotor VTOL UAV," *60th Annual Forum of the American Helicopter Society*. 574
- [19] Akturk, A., and Camci, C., 2011, "Tip Clearance Investigation of a Ducted Fan Used in VTOL UAVs—Part I: Baseline Experiments and Computational Validation," *Proceedings of ASME Turbo Expo 2011: Power for Land, Sea and Air*, GT2011-46356. 575

549

550

551

552

553

554

555

556

560 AQ17

561

562

563 AQ18

564

565

566

567

568

569

570

571

572

573

574

575

576

577

578

579

580 AQ19

581

582 AQ20

583

584

585 AQ21

586

587

588

589

590